Transport of *Cryptosporidium parvum* in porous media: Long-term elution experiments and continuous time random walk filtration modeling

Andrea Cortis,[1,2] Thomas Harter,[1] Lingling Hou,[3] E. Robert Atwill,[3] Aaron I. Packman,[4] and Peter G. Green[5]

Received 14 January 2006; revised 3 May 2006; accepted 29 June 2006; published 12 October 2006.

[1] Complex transport behavior other than advection-dispersion, simple retardation, and first-order removal has been observed in many biocolloid transport experiments in porous media. Such nonideal transport behavior is particularly evident in the late time elution of biocolloids at low concentrations. Here we present a series of saturated column experiments that were designed to measure the breakthrough and long-term elution of *Cryptosporidium parvum* in medium sand for a few thousand pore volumes after the initial source of oocysts was removed. For a wide range of ionic strengths, I, we consistently observe slower-than-Fickian, power law tailing. The slope of the tail is flatter for higher I. At very high ionic strength the slope decays to a rate slower than t^{-1}. To explain this behavior, we propose a new filtration model based on the continuous time random walk (CTRW) theory. Our theory upscales heterogeneities at both the pore-scale geometry of the flow field and the grain surface physicochemical properties that affect biocolloid attachment and detachment. Pore-scale heterogeneities in fluid flow are shown to control the breakthrough of a conservative tracer but are shown to have negligible effect on oocyst transport. In our experiments, *C. parvum* transport is dominated by the effects of physicochemical heterogeneities. The CTRW model provides a parsimonious theory of nonreactive and reactive transport. The CTRW filtration process is controlled by three parameters, Λ, β, and c, which are related to the overall breakthrough retardation ($R = 1 + \Lambda$), the slope of the power law tail (β), and the transition to a slower than t^{-1} decay (c).

Citation: Cortis, A., T. Harter, L. Hou, E. R. Atwill, A. I. Packman, and P. G. Green (2006), Transport of *Cryptosporidium parvum* in porous media: Long-term elution experiments and continuous time random walk filtration modeling, *Water Resour. Res.*, *42*, W12S13, doi:10.1029/2006WR004897.

1. Introduction

[2] Waterborne diseases are among the most prevalent health issues in many developing countries, and are also of concern in developed countries around the world (http://www.unesco.org/water/wwap/facts_figures/basic_needs.shtml). The environmental fate of waterborne pathogens, particularly those that are largely resistent to chlorination, such as *Cryptosporidium parvum* and *Giardia duodenalis* spp., are of significant concern. While the risk of microbial contamination from fecal matter, wastewater, etc. is most prevalent in surface waters, groundwaters are critically affected as well [*Lisle and Rose*, 1995; *Hancock et al.*, 1998].

[3] Worldwide, groundwater is an important source of drinking water. In rural areas, domestic wells provide much of the (untreated) drinking water supply. For example, 25% of households in the United States and 30% of households in Canada (http://www.ec.gc.ca/water/en/info/facts/e_domestic.htm) rely on domestic wells for their water supply. In Europe, and increasingly also in the United States, municipal water purveyors rely on bank filtration (groundwater pumping in the immediate vicinity of a stream) for pathogen removal from surface water sources [*Cote et al.*, 2002].

[4] Pathogen filtration in streambeds during hyporheic exchange is another key process controlling stream water quality [*Ren and Packman*, 2002]. Some bacteria also play an important role in mitigating the effects of subsurface contamination. Recent reviews [*Harvey and Garabedian*, 1991; *Ryan and Elimelech*, 1996; *Ginn et al.*, 2002] bear witness to current interest in the fate of so-called biocolloids

[1]Department of Land, Air, and Water Resources, University of California, Davis, California, USA.
[2]Now at Earth Science Division, Lawrence Berkeley National Laboratory, Berkeley, California, USA.
[3]Department of Population Health and Reproduction, Veterinary Medicine Teaching and Resource Center, University of California, Davis, Tulare, California, USA.
[4]Department of Civil and Environmental Engineering, Northwestern University, Evanston, Illinois, USA.
[5]Department of Civil and Environmental Engineering, University of California, Davis, California, USA.

0043-1397/06/2006WR004897$09.00

(viruses, bacteria, and the (oo)cysts of, e.g., the parasitic protozoa *C. parvum* and *Giardia* spp.).

[5] Understanding late time elution of *C. parvum* oocysts is critical because these dormant oocysts may remain infective for extended periods of time unlike many other microbial contaminants. Experiments involving immersion in river water indicate that half of the oocysts' population remains infective after ~30 days [*Robertson et al.*, 1992]. Oocysts may survive in various environments for many months [see, e.g., *Walker et al.*, 1998]. Furthermore, *C. parvum* is released into groundwater recharge at concentrations of 10^5 to 10^6 oocysts per liter [*Bradford and Schijven*, 2002; *Schijven et al.*, 2004], yet it remains infectious and potentially lethal for humans after ingestion of a few oocysts [*Okhuysen et al.*, 1999].

[6] The transport of *C. parvum* and other colloidal particles in porous media is attributed to four major mechanisms: advection, dispersion, straining, and physicochemical particle-surface interactions [*McDowell-Boyer et al.*, 1986; *Ryan and Elimelech*, 1996]. Advection and dispersion describe the transport of colloidal particles within the water phase of a porous medium. Straining is the permanent physical trapping of colloidal particles in pore throats that are too small to allow passage. Straining is a major removal process in porous media with grain diameters smaller than 20–50 times the biocolloid diameter [*de Marsily*, 1986; *McDowell-Boyer et al.*, 1986].

[7] Physicochemical interactions with the porous medium occur when *C. parvum* oocysts approach grain surfaces due to pore-scale diffusion, sedimentation, or inertial forces [*McDowell-Boyer et al.*, 1986]. Colloid surface interactions lead to permanent or temporary attachment to the solid phase of the porous medium. Colloid interactions with grain surfaces are controlled by electrostatic forces including London–Van der Waals forces. Electrostatic forces between colloids and grain surfaces are explained by the so-called electric double-layer theory [see, e.g., *Israelachvili*, 1991]. Particles are known to deposit in the secondary energy minimum of the electric double layer at the grain surface. Deeper secondary minima at closer range to the solids surface occur at higher ionic strength [*Redman et al.*, 2004]. Hence changes in the solution chemistry promote colloid mobilization (deposition) by altering the double layer potential energy.

[8] *C. parvum* oocysts are negatively charged with a small ζ potential on the order of -10 mV. The negative charge most likely results from proteins on the oocyst surface that extend into the solution [*Kuznar and Elimelech*, 2004, 2005]. Cations in solution cause charge neutralization of surface proteins. Conformational changes caused by charge neutralization may cause the collapse of proteins and lead to the elimination of steric repulsion. Thus the range of electrostatic interactions is reduced yielding higher oocyst attachment efficiency [*Kuznar and Elimelech*, 2004]. For example, *Kuznar and Elimelech* [2005] reported that the deposition rate of the oocysts onto a quartz substrate was doubled after 1 hour exposure to heat at 80°C. The increase in attachment efficiency was attributed to denaturation of proteins on the oocyst surface, because the heat treatment did not significantly change the ζ potential of the oocysts. The negatively charged oocysts may attach to negatively charged surfaces, such as those of round pure quartz sand grains, due to the presence of surface heterogeneities at the grain scale [*Song et al.*, 1994]. Heterogeneity of the density of electrostatic surface charges and of their polarity have been attributed to physical and chemical imperfections, e.g., cracks, edges, lattice defects, and chemical impurities [*Johnson et al.*, 1996].

[9] Given these processes, breakthrough curves (BTCs) of *C. parvum* and other biocolloids in the laboratory and in field experiments with finite-period injections typically show five distinct periods as described by *Johnson et al.* [1995]: The first period (A) identifies the time after injection, but prior to any breakthrough. The second period (B) identifies the rising limb in the breakthrough curve. During the third period (C), concentration reaches a steady state plateau if the injection is also steady and has a sufficient duration. Some time after the injection has terminated, the outflow concentration will rapidly decrease (fourth period, D). Finally, a period (E) of nonzero concentrations at a more or less consistent "elution plateau" will begin as the the breakthrough changes from representing advection-dominated transport to representing attachment-detachment-dominated transport. The nature of this "elution plateau" has not been fully investigated, as most of the reported biocolloid elution experiments are terminated after a few pore volumes. However, many reported experiments with *C. parvum* and other biocolloids show a distinct transition to an "elution plateau" period E just prior to termination of the experiment [see, e.g., *Johnson et al.*, 1995; *Camesano et al.*, 1999; *Johnson et al.*, 2005; *Bradford and Bettahar*, 2005]. These experiments suggest the existence of a late time tail, but little is known about the characteristics of this tail. *Harter et al.* [2000] shows an example of a late time elution curve, measured over a dynamic range of three orders of magnitude and extending over 200 pore volumes after termination of injection. In that work, the tail was approximated by means of a first-order kinetic sorption-desorption filtration model.

[10] In this paper we seek to shed further light on the late time elution of *C. parvum*. We implement several column experiments with varying ionic strength. We propose a generalized model based on CTRW theory [see *Berkowitz et al.*, 2006, and references therein] that adequately captures all five characteristic periods including the elution tail of the measured BTCs without increasing the number of fitting parameters relative to the traditional reactive advection-dispersion filtration models used, for example, by *Harter et al.* [2000] and *Bradford and Bettahar* [2005].

2. Experimental Methods

2.1. Collection and Purification of *C. parvum* Oocysts

[11] Feces were collected from naturally infected calves at 9–21 days of age from three local commercial dairies in Tulare, California, which served as the source of wild-type *C. parvum* oocysts for these experiments. These oocysts were previously classified as bovine genotype A, using the genotyping scheme described by *Xiao et al.* [1999]. Using an acid fast protocol to detect oocysts [*Harp et al.*, 1996], samples having more than 25 oocysts per 400 microscopic field on fecal smears were washed through a series of 40, 100, 200, and 270 mesh sieves with Tween water (0.2% Tween 20 in deionized water [vol/vol]). The resulting

suspension was centrifuged at 1500 g for 20 min in a 250 mL centrifuge tube, supernatant discarded and the pellet diluted in Tween water. Discontinuous sucrose gradients were used to purify *C. parvum* oocysts from fecal suspensions [*Arrowood and Sterling*, 1987]. Purified oocysts were stored in storage solution which contained 0.001% Amphotericin, 0.006% Penicillin G, 0.01% Streptomycin Sulfate, and 0.01% Tween 20 [*Hou et al.*, 2004]. Using a phase contrast hemacytometer (bright line hemacytometer: Hausser Scientific, Horsham, Pennsylvania), concentrations of purified oocysts were determined as the arithmetic mean of 8 independent counts. Oocysts were used within 2–7 days of fecal collection.

2.2. Column Experiments

[12] Four experiments were implemented in two replicate Plexiglas columns. Columns were 5.1 cm in inner diameter and 20 cm in length. The porous medium used was Accusand Filtration Sand (Mesh 30/40, UNIMIN Corporation, Ottawa, Minnesota) that was washed, dried, and sieved. Columns were wet-packed firmly and saturated with degassed deionized water (DIW) followed by washing with 10 pore volumes (p.v.) of degassed DIW. The pore volume was computed based on the total dry weight of packed sand, the total column volume, and the specific density of the Ottawa sand used in the experiments (2.65 g/cm^3). The total measured outflow from the column experiments at a given time is divided by the computed pore volume to obtain dimensionless units of time. Experimental solutions were prepared by dissolving NaCl or MgCl in DIW to the desired ionic strength followed by degassing. The oocyst solution was obtained by spiking an aliquot of the experimental solution to a concentration of 10^6 oocyst/mL. For the column experiment, a constant flow rate of 10 mL per minute was established; then 2.5 pore volumes of 50 mg/L NaBr solution was injected into the column (tracer experiment). Effluent water was continuously collected in one minute intervals for 60 min. The columns were then washed with the desired experimental solution for at least 10 p.v. before oocyst injection. Without flow interruption, the oocyst injection occurred over 2.5 p.v., followed by 1600 to 2400 p.v. of oocyst free solution injection. Outflow was continually collected at one minute intervals for first 60 min, then 10 mL aliquots were collected at 60, 180, 360 and 720 min intervals.

2.3. Determining the Concentration of *C. parvum* Oocysts in Aliquots of Column Water

[13] One hundred and ten microliters of Tween 80 were added to each column water sample, resulting in a 0.1% Tween 80 solution. To enumerate oocysts samples from the plateau phase (period C), samples were diluted 1:100. Samples from period B, D, and E (tail) were concentrated hundredfold by centrifuging for 10 min at 1000 g, supernatant discarded and the pellet resuspended in 0.1 water. Ten microliters of suspension were smeared onto a commercially prepared glass slide and air-dried overnight. A positive and negative control was included for each set of slides. A direct immunofluorescent assay was performed using a commercial kit (Cryptosporidium/Giardi direct immunofluorescent detection kit A 400 FL CryptoaGloTM, WaterborneTM, Inc., New Orleans, LA) with an Olympus BX60 microscope at 400X magnification. All oocysts were enumerated for each 10 μl subsample and depending on the process sued for the original aliquot of column water (dilution or concentration), a crude estimate of oocysts per mL calculated from this value. This crude concentration of oocysts was adjusted for the percent recovery of the direct immunofluorescent assay by first spiking two different solutions, boiled distilled water and 15 mM NaCl, with purified *C. parvum* oocysts to a final concentration of 10^5 oocysts/ml. Each solution was then passed through the column apparatus but without soil and processed as above. Four replicate enumerations were performed for each solution. Negative binomial regression was used to estimate the percent recovery and 95% confidence interval [*Atwill et al.*, 2003].

2.4. Bromide Analysis

[14] All bromide samples were analyzed with an ion selective electrode (quantitation limit: 1 mg/L). In one experiment, samples of the entire outflow experiment (tracer and oocyst elution) were analyzed for dissolved bromide using an ICP-MS (model 7500i, Agilent, Palo Alto, California). Samples were introduced with 1.1 l/min Ar through a Babbington nebulizer at 0.4 mL/min and into a thermoelectrically cooled double-pass spray chamber (2°C) and then into a robust 1400 W plasma for ionization. NIST traceable standards were used for external calibration and prepared in 18.2 MOhm $\times$ cm resistivity UV oxidized and sterilized water with TOC < 10 ppb (MilliQ A10, Millipore Corp, Billerica, Massachusetts). Standards were analyzed from 0.1 ng/mL (ppb), which is below the detection limit, up through 100 mg/L (ppm). With probe rinsing and rinse bottle uptake at the autosampler between every analysis, a linear quantitative working range of more than 4 orders of magnitude was achieved. The minimum instrumental detection limit was $\sim$1 ppb while the method quantitation limit was $\sim$10 ppb.

3. Theory

3.1. Reactive Advection Dispersion Model With Filtration

[15] The transport behavior of biocolloids is commonly modeled by colloid filtration theory (CFT) [*Yao et al.*, 1971] as an extension of the common advection-dispersion equation. CFT has been found a useful model in many applications ranging from fabricated filter systems to biocolloid transport.

[16] The advection-dispersion-filtration equation reads:

$$\frac{\partial c}{\partial t} = -v\left[\lambda c + \frac{\partial c}{\partial x} - \alpha\frac{\partial^2 c}{\partial x^2}\right] \tag{1}$$

where v is the pore velocity [L/T], α is the dispersivity [L], and λ [L^{-1}] is the so-called filtration coefficient (assumed to be constant in time and space). CFT provides a conceptual framework to compute λ from physical properties of the colloid and the porous medium:

$$\lambda = \frac{3}{2}(1-\theta)\frac{L}{d_c}\alpha_c\eta \tag{2}$$

where α_c is the collision efficiency, θ is the porosity, η is the collector efficiency, d_c is the median grain size diameter

[*Rajagopalan and Tien*, 1976], and L is the length of the column. α_c is an empirical (fitting) constant while η can be computed based on the physical conditions of the experiment. Expressions for η are reviewed by *Logan et al.* [1995] and by *Tufenkji and Elimelech* [2004].

[17] This model assumes particle and grain (collector) homogeneity at all length scales and predicts a fast exponential concentration decay along the colloid travel path of the form

$$\frac{dc}{dx} = -\frac{c}{\ell}, \tag{3}$$

where $\ell \equiv \lambda^{-1}$ is a characteristic filtration length scale. This model adequately describes the initial advection-dispersion dominated breakthrough (periods A–D), but does not provide a conceptual framework for late time elution of biocolloids (period E).

[18] To account for the occurrence of nonideal behavior, (1) has sometimes been combined with a model for a first-order, rate-limited adsorption-desorption process [*Toride et al.*, 1995]

$$\frac{\partial c}{\partial t} + \frac{\rho_b}{\theta}\frac{\partial s}{\partial t} = -v\left[\lambda c + \frac{\partial c}{\partial x} - \alpha\frac{\partial^2 c}{\partial x^2}\right], \tag{4a}$$

$$\frac{\partial s}{\partial t} = \frac{\theta}{\rho_b} k_f c - k_r s \tag{4b}$$

where ρ_b is the colloid density, s is the concentration of *C. parvum* oocysts adsorbed reversibly on solid surfaces, and k_f, and k_r are the forward and reverse sorption rates, respectively.

[19] This reactive ADE ("RADE") filtration model was first proposed for oocyst transport in porous media by *Harter et al.* [2000]. [*Bradford and Bettahar*, 2005] used the same mathematical form, but attributed permanent removal of oocysts solely to physical straining and interpreted k_f in (4b) to be identical to our λ in (2). More generally, *Johnson et al.* [1995] proposed that both, a time-dependent detachment function and a degree of sorption site heterogeneity are required to describe bacterial attachment and detachment during transport.

[20] All modifications of this standard filtration model predict an exponential decay of the oocyst concentration. Power law tails in the BTCs cannot be modeled with filtration theory or the modifications presented above. Furthermore, deviations from the log linear profile predicted by (3) have been observed [*Albinger et al.*, 1994; *Martin et al.*, 1996; *Camesano and Logan*, 1998; *Baygents et al.*, 1998; *Bolster et al.*, 1999; *Redman et al.*, 2001b; *Johnson et al.*, 2005]. Several of these report concentration profiles that strongly resemble a power law.

3.2. CTRW-Based Filtration Model

[21] The starting point of our theory is the observation that physicochemical attachment and detachment can be attributed to small scale heterogeneities at the level of the pore scale. In particular, surface charge heterogeneities on both, the oocyst and the solids phase play a fundamental role in the transport of colloidal particles. Furthermore, oocysts and other biocolloids can vary in shape, size, surface chemistry, and surface heterogeneity, even if only within a relatively narrow range. It is not feasible to obtain detailed knowledge of the microscopic features of these heterogeneities at the pore and oocyst individuum level. We therefore suggest to treat heterogeneities in a stochastic framework and upscale by ensemble average to the scale of the experiment.

[22] CTRW is a stochastic transport theory based on local-scale ensemble averages. At the heart of the CTRW formulation is $\psi(\mathbf{s}, t)$, the probability density function (pdf) for a single transition over space $\mathbf{s}$ and time t. This function is general and can implicitly represent transport by any mechanism (e.g., advection, dispersion, sorption, and desorption) that displaces a particle from one spatial location to another (separated by $\mathbf{s}$) during a finite time interval t. Power law tails of passive tracer experiments in porous media have been successfully described in the framework of the CTRW theory [*Berkowitz and Scher*, 1995; *Cortis et al.*, 2004a; *Cortis and Berkowitz*, 2004; *Jiménez-Hornero et al.*, 2005].

[23] In this section we formulate a description of the advection-dispersion with attachment and detachment typical of the experiments described in section 2. Our theory follows closely the theory first proposed by *Margolin et al.* [2003]. There adsorption and desorption processes are defined by means of a "sticking rate" and a "sticking time" pdf. In our experiments the nonsorbing phase is the aqueous solution and the sorbing (colloidal) phase is *C. parvum*.

[24] The $\psi(\mathbf{s}, t)$ is split into two distinct components: one related to the complexity of the pore space geometry, $\psi_0(\mathbf{s}, t)$, and a second one which defines the retention of colloidal particles, $\phi(t|\tau)$, where $\tau = (t - t')/T$. In this formulation, colloidal particles are considered to be temporarily trapped or retained at position $\mathbf{s}$ for some time t. The final $\psi(\mathbf{s}, t)$ is given by a generalized convolution integral of the two contributions:

$$\psi(\mathbf{s}, t) = \int_0^t \psi_0(\mathbf{s}, t - t')\phi(t'|t - t')dt'. \tag{5}$$

If $\phi(t|\tau)$ pdf is very narrow, CTRW more closely resembles the reactive ADE. In the limit $\phi(t|\tau) \equiv \delta(t' - \Lambda\tau)$, we obtain the ADE with simple retardation $R = 1 + \Lambda$ [*Margolin et al.*, 2003].

[25] More generally, $\phi(t|\tau)$ accounts for multiple attachment and detachment events of a tracer particle in the time interval τ. Thus $\phi(t|\tau)$ can be defined by means of a compound Poisson process, i.e., multiple convolutions of a large number of single "sticking time" pdfs, $\varphi(\mathbf{s})$, where the sticking time is the time between attachment and detachment. Assuming that in the free state there exists a sticking probability per unit time, Λ, we can construct

$$\tilde{\phi}(u, \mathbf{s}) \equiv e^{\Lambda\tau(\varphi(u)-1)}, \tag{6}$$

where the symbol ˜ indicates Laplace transformed quantities with respect to time t and u is the Laplace variable. The parameter Λ represents a measure of the average sticking

rate. With these definitions it is possible to define a new function $\nu(u)$

$$\nu(u) \equiv u + \Lambda(1 - \tilde{\varphi}(u)), \tag{7}$$

such that

$$\tilde{\psi}(\mathbf{s}, u) = \tilde{\psi}_0(\mathbf{s}, \nu(u)). \tag{8}$$

Margolin et al. [2003] discuss two main forms of the sticking time pdf $\tilde{\varphi}(u)$ namely, a "narrow" (exponential) form, $\tilde{\varphi}(u) \approx 1 - \bar{t}u$, and a "broad" (power law) form $\tilde{\varphi}(u) \approx 1 - cu^{\beta}/\Lambda$. Also in these cases one can define an asymptotic retardation $R = 1 + \Lambda\bar{t}$. A thorough account of these developments can be found in the work of *Margolin et al.* [2003].

[26] Following *Berkowitz et al.* [2002], *Cortis et al.* [2004b], and *Dentz et al.* [2004], it is possible to show that an expansion of the classical equations for the CTRW yields a partial differential equation (written in the Laplace space)

$$u\tilde{c}(\mathbf{x}, u) - c_0(\mathbf{x}) = -\tilde{M}(u)v_{\psi}\left[\frac{\partial}{\partial x}\tilde{c}(\mathbf{x}, u) - \alpha_{\psi}\frac{\partial^2}{\partial x^2}\tilde{c}(\mathbf{x}, u)\right] \tag{9}$$

where

$$\tilde{M}(u) = \bar{t}u\frac{\tilde{\psi}(u)}{1 - \tilde{\psi}(u)} \tag{10}$$

is a memory function and $\tilde{\psi}(\mathbf{s}, u) \equiv p(s)\tilde{\psi}(u)$. The generalized velocity v_{ψ} and dispersivity α_{ψ} are defined by $v_{\psi} = \bar{t}^{-1}\sum_s p(s)s$ and by $\alpha_{\psi} = \frac{1}{2}\bar{t}^{-1}\sum_s p(s)s^2$, which are the first and second moment of $p(s)$, respectively.

[27] A generalization of (9) is obtained by introducing a permanent filtration deposition term proportional to the colloidal concentration flux:

$$u\tilde{c}(\mathbf{x}, u) - c_0(\mathbf{x}) = -\tilde{M}(u)v_{\psi}[\lambda\tilde{c}(\mathbf{x}, u) + \frac{\partial}{\partial x}\tilde{c}(\mathbf{x}, u) - \alpha_{\psi}\frac{\partial^2}{\partial x^2}\tilde{c}(\mathbf{x}, u)]. \tag{11}$$

The main difference between (11) and classical filtration theory is that the RHS of the filtration equation (1) is convoluted in time with the memory function $\tilde{M}(u)$. This is consistent with the requirement of a time-dependent filtration coefficient reported by *Johnson et al.* [1995] and also consistent (though not completely equivalent) with fractal filtration theory [*Redman et al.*, 2001a, 2001b]. Equation (11) properly represents the effect of kinetic attachment-detachment behavior by explicitly relating microscale to macroscale behavior.

[28] To analyze our column experiments, we will consider the one-dimensional form of (11) and rescale the spatial coordinate x by the length of the column $x \rightarrow x/L$, i.e., $x \in [0, 1]$. The time is rescaled by a characteristic time $t \rightarrow t/\bar{t}$ so that the fluid velocity $v = 1$, i.e., time can be replaced by pore volumes. The Laplace variable is made nondimensional by $u \rightarrow u\bar{t}$.

[29] At this point we introduce some assumptions on the functional forms of $\psi_0(t)$ and $\varphi(t)$. *Cortis et al.* [2004a] have shown that CTRW can account for the anomalous tailing in the breakthrough of conservative tracers in homogeneously packed soil columns. The $\psi_0(t)$ defined by *Cortis et al.* [2004a] captures the late time nonideal transport due to pore shape heterogeneity. In our passive tracer experiments, the asymmetry of the tail is too small to be captured by the particular form of $\psi_0(t)$ suggested by *Cortis et al.* [2004a], i.e., the measured BTC is almost Gaussian. To account for pore level geometric heterogeneity of our experiments, it is sufficient to use an asymptotic power law model $\tilde{\psi}_0(u) = 1/(1 + u^{\gamma})$. For homogeneous porous media, γ tends to 1. In the limit $\gamma \rightarrow 1$, transport follows a Fickian-type advection-dispersion behavior, i.e., the pdf distribution decays like an exponential, $\psi_0(t) = \exp(-t/\bar{t})$, i.e., $\tilde{\psi}_0(u) = 1/(1 + u)$.

[30] Small-scale heterogeneities in physicochemical interactions are represented by a sticking time pdf in the form:

$$\tilde{\varphi}(u) \equiv \frac{1}{1 + u^{\beta}}, \tag{12}$$

where the exponent β is positive and smaller than one. This formulation yields power law tailing. From a physical point of view, this means that there is no characteristic filtration timescale for this problem. This is consistent with the observations of *Redman et al.* [2001a] and *Tufenkji et al.* [2004] of a power law distribution of filtration lengths. Note that the splitting of the convolution integral introduced in (5) provides a means to assess the validity of the theory by comparing experiments with nonreactive tracers to those with colloids.

[31] A slower than t^{-1} decay cannot be modeled with the power law function postulated in (12). We call this a "flat elution plateau". This flat elution plateau can be represented by a uniform distribution $\tilde{\varphi}(u) \equiv (Tu)^{-1}$, where T represents the truncation time for the distribution, i.e., the maximum observation time for the BTC. From a physical point of view this means that the jump events in the system do not show any organized behavior.

[32] We postulate that the $\tilde{\varphi}(u)$ describing our experiments takes the combined form

$$\tilde{\varphi}(u) = c\frac{1}{1 + u^{\beta}} + (1 - c)\frac{1}{Tu}, \tag{13}$$

where the parameter c sets the relative importance of the power law versus uniform behavior. The final expression for $\tilde{\psi}(u)$ for the particular choice of $\tilde{\varphi}(u)$ in (13) thus reads

$$\tilde{\psi}(u) = \left[1 + u + \Lambda\left(1 - c\frac{1}{1 + u^{\beta}} - (1 - c)\frac{1}{Tu}\right)\right]^{-1}. \tag{14}$$

When $\Lambda = 0$ (i.e., $\tilde{M}(u) = 1$) and $\lambda = 0$, equation (11) is equivalent to the classical ADE for passive solute transport. When $\tilde{M}(u) = 1$, $\Lambda = 0$ and $\lambda > 0$ the equation reduces to the classical filtration theory. If $\Lambda > 0$, the memory $\tilde{M}(u) \neq 1$, i.e., the filtration equation is convoluted with the memory function $\tilde{M}(u)$.

4. Results and Discussion

4.1. CTRW Filtration Model

[33] In Figures 1a–1e we present a series of numerical simulations to demonstrate the effect of the various param-

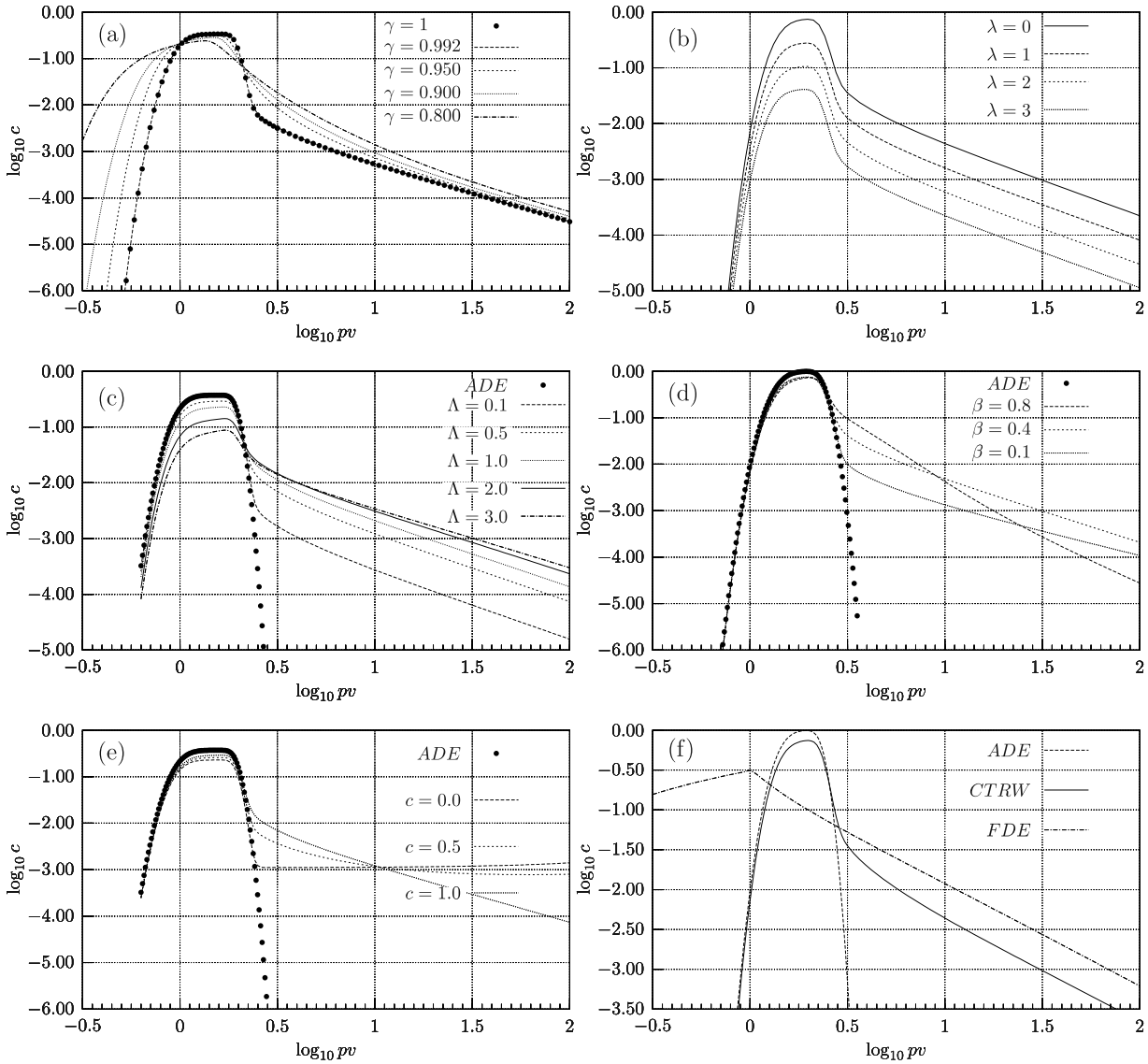

Figure 1. Effect of the various parameters entering the CTRW transport formulation. For Figures 1a–1f, $v_\psi = 1$, $\alpha = 0.01$, and the duration of the injection was set equal to one pore volume, i.e., the inlet BC for the flux averaged concentration (in the Laplace space) was set equal to $\tilde{c}_f(u) = (1 - \exp(-u))/u$. (a) Effect of the exponent γ (representing geometric disorder) for $\beta = 0.3$, $\Lambda = 0.2$, $\lambda = 1$, and $c = 1$; (b) effect of the filtration coefficient λ for $\beta = 0.35$, $\lambda = 0.4$, and $c = 1$; (c) effect of the sticking coefficient Λ for $\beta = 0.3$, $\Lambda = 0.5$, and $c = 1$; (d) effect of the anomalous exponent β (representing physical-chemical disorder) for $\Lambda = 0.4$, $\lambda = 0$, and $c = 1$; (e) effect of the weighting coefficient c (power law versus flat tail behavior) for $\beta = 0.3$, $\lambda = 0.5$ and $\lambda = 1$; (f) comparison of the CTRW model with the classical advection dispersion equation (ADE) model and the fractional-in-time derivative (FDE) model.

eters of the CTRW Filtration equation (11). The simulations present the outflow concentrations of a hypothetical sand column experiment. The boundary condition at the inlet is a unit duration pulse of unit relative concentration. In Laplace space, the flux-averaged concentration at the inlet is $\tilde{c}_0(x = 0, u) = (1 - \exp(-u))/u$. The boundary condition at the outlet, $x = L$, is of the Neumann type, $d\tilde{c}_0(x = L, u)/dx = 0$. The column has a nondimensional unit length, $L = 1$, and time units are in "pore volumes," imposing a nondimensional velocity $v_\psi = 1$. Unless noted otherwise, the parameters used for these hypothetical simulations are $\alpha = 0.01$ (nondimensional dispersivity), $\gamma = 1$ (no geometrical disorder), $\lambda = 0$ (no filtration), $\Lambda = 0.4$, $\beta = 0.3$, and $c = 1$.

[34] Figure 1a demonstrates the effect of geometrical disorder among individual pores of the porous medium ($\gamma < 1$) on the transport of oocysts. Greater heterogeneity in the geometric arrangement of the pore space leads to earlier solute arrival (period B), stronger asymmetry in the peak breakthrough (period C), and higher concentrations in the tail of the BTC (period E).

[35] The filtration coefficient, λ, accounts for permanent removal of colloids in the column experiment (Figure 1b). In log-log space, λ rescales most of the breakthrough curve

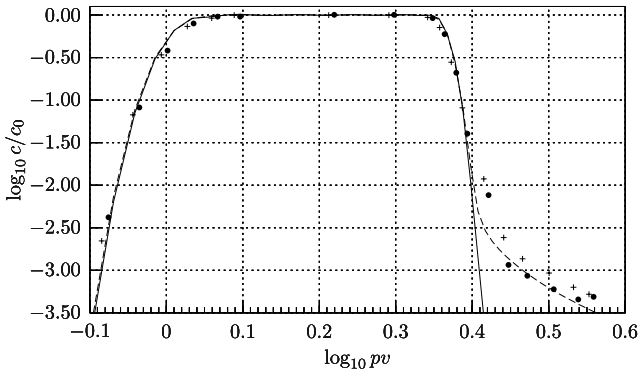

Figure 2. Bromide tracer experiment. The injected volume was 1.5 pore volumes. Solid line represents the ADE model. Dashed line represents the CTRW model with a $\tilde{\psi}_0(u) = 1/(1 + u^{\gamma})$ and $\gamma = 0.9992$. Compare with Figure 1a.

by a constant amount. After the initial increase in oocyst concentrations (period B), the difference in log-concentration levels between BTCs of different λ are constant for the remainder of the experiment (periods C, D, E). The difference in the logarithm of the concentration is proportional to the difference in λ. Larger filtration coefficients reflect stronger permanent removal in the column and, hence lower eluent concentration. However, the magnitude of the concentration decrease during period D and the slope of the tail in period E are unaffected by the filtration coefficient.

[36] The sticking coefficient, Λ, is a measure of the average sticking time of the colloids. Larger Λ increases the asymmetry in breakthrough by reducing the initial transport through the column and extending the tail (Figure 1c). Also, with increasing Λ, the transition point from period D to E occurs earlier and the entire tail concentration (period E) shifts upward. At very large Λ, the initial slope in period E is flatter than the asymptotic value at late time. The asymptotic slope of the tail at large t is unaffected by the magnitude of Λ.

[37] The power law slope of the BTC tail (period E) is controlled by β, which has a value between 0 and 1. The effect of this parameter is shown in Figure 1d. The power law tailing extends to $t \rightarrow \infty$. In the absence of heterogeneity in the pore geometry, the β coefficient (and any other parameter entering the expression for the memory function $\tilde{M}(u)$) are intrinsically determined by the nature of the distribution of the colloid attachment and detachment events. The flattest slope that can be modeled with a power law is equal to -1, i.e., $\beta = 0$.

[38] Changes in β do not affect the total mass of colloids eluted over time; the irreversible deposition of oocysts is controlled strictly by the filtration coefficient λ. The impact of β on the peak concentration (period C) varies depending on the choice of other parameters. In the example given in 1c, a small decrease in peak concentration occurs as β increases.

[39] Note that negative values for β (i.e., tailing slower than t^{-1}) are physically implausible as the integral $\int_0^{\infty} \psi_0(t)dt$ diverges for $\beta \leq 0$. (Values of $-1 < \beta < 0$ are allowed for the truncated power law model [*Dentz et al.*, 2004]). Tails with a decay slower than t^{-1} ("flat tails") indicate that the tail is of finite temporal extent, otherwise the mass eluted would be infinite ($c < 1$, Figure 1e). The proposed model assures a smooth transition from power law behavior at the onset of period E to a relatively flat tail in the later part of period E. Smaller c characterizes faster transition to a flat tail. In the examples shown in Figure 1e, the tail is truncated at 100 pore volumes.

[40] In Figure 1f we show the comparison between our model, the classical ADE, and the fractional derivative in time (FDE) model, which has recently been proposed as an alternative approach to the classical ADE. The FDE is characterized by a $\psi_0(t) = 1/(1 + u^{\beta})$, i.e., is a subset of the more general CTRW formulation [*Berkowitz et al.*, 2006]. While the tail of the FDE reproduces a power law behavior, it does not accurately represent the early breakthrough. The value of β is 0.35 for both the FDE and (11) models. The remaining parameters of (11) were $c = 1$ (i.e., pure power law tailing), the filtration coefficient $\lambda = 0$ (i.e., no irreversible attachment) and $\Lambda = 0.4$. Unlike the CTRW model, the fractional derivative equation cannot simultaneously account for both the early ADE-like shape of the BTC and the power law tail in the elution curve.

4.2. Experimental Results and Model Fits

[41] A passive tracer (bromide) experiment was performed for each of the porous columns of our study. The packing procedure adopted in the present work is very similar to the one used by *Cortis et al.* [2004a]. Passive tracer experiments with a NaBr solution yielded ADE type behavior when analyzed over a dynamic range of less than two orders of magnitude. Slight tailing was observed in the samples analyzed with the ICP-MS (four orders of magnitude dynamic range). Tailing was observed only after concentrations decreased exponentially by nearly three orders of magnitude (see Figure 2). This behavior is consistent with the results found by *Cortis et al.* [2004a], who used columns of comparable length but only half the diameter size (i.e., had a smaller averaging volume, resulting in a wider range of γ). The $\tilde{\psi}(u) = 1/(1 + u^{\gamma})$ provides an excellent fit to the bromide breakthrough curve in Figure 2. The pure ADE model prediction ($\gamma = 1$) is identical with that of the CTRW model throughout the peak but does not capture the onset of tailing. The slope of the power law tail is very steep (approximately six) yielding an exponent γ that is only slightly smaller than 1 ($\gamma = 0.9992$). This degree of nonideality is common to so-called "homogeneous" column experiments and has been shown to be due to heterogeneities in pore geometry [*Cortis et al.*, 2004a]. Note that the proposed formalism can be easily adjusted to other forms of geometrical disorder that would affect ideal tracer transport [*Cortis et al.*, 2004a].

[42] While important for the prediction of the tailing behavior of the conservative tracer, the amount of geometric disorder is too small to significantly influence the behavior of the reactive colloids. As shown in Figure 1a, the colloid BTC for $\gamma = 0.9992$ is indistinguishable from that for $\gamma = 1$. For purposes of modeling colloid BTCs (in the parameter range comparable to that in Figure 1a), it is therefore appropriate to neglect the geometric pore-space disorder and assume that the advective-dispersive contribution to colloid transport follows a traditional ADE with $\tilde{\psi}_0(u) = 1/(1 + u)$.

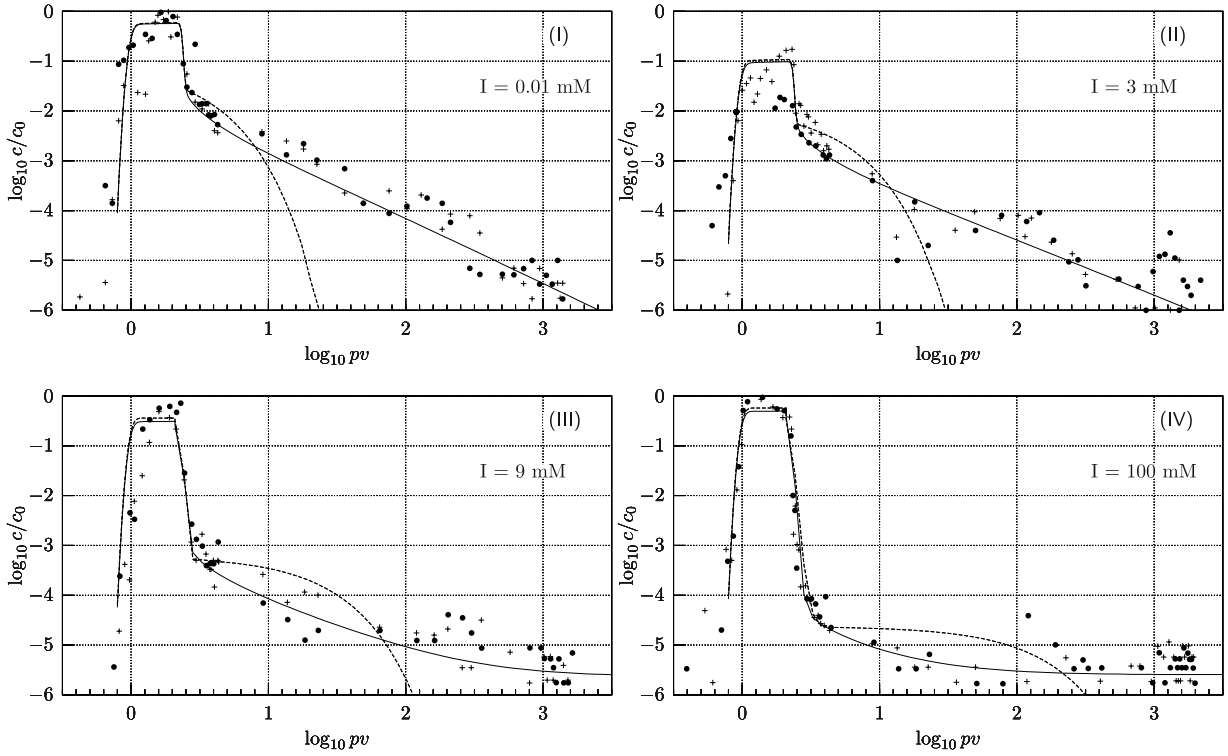

Figure 3. Experimental BTC for the oocyst elution at different ionic strength *I*. Injection volume was set equal to 1.5 pore volumes. Dots and crosses represent the two replica for each elution experiment. Solid line represents the CTRW model (11), with (14). Dashed line represents the RADE model (4). The parameters for the two models are reported in Table 1.

[43] Dispersivity was fitted to the rising limb of the bromide BTC (period B). The dimensional value for the dispersivity was found to be $\alpha \times L = 0.002 \times 0.20 = 4 \times 10^{-4}$ m, a value comparable to the mean diameter of the sand grains, $d_c = 2.75 \times 10^{-4}$ m (see Figure 2). This dispersivity is typical for sand column experiments [*Cortis et al.*, 2004a].

[44] Results from the *C. parvum* experiments are shown in Figure 3. Data for the two replicate experiments are shown separately to indicate the experimental variability between replicates. The imposed volumetric flux was 10 mL/min which represents a relatively high interstitial pore velocity relative to typical regional groundwater fluxes. Such high pore velocities are characteristic of near-well conditions and of conditions in the hyporheic zone of a streambed [*Ren and Packman*, 2002]. Concentrations shown are normalized with respect to the input concentration, $c_0 = 10^6$ oocysts/mL.

[45] In experiments I, II, and IV (see Figure 3), the oocysts were diluted in NaCl solutions with 0.01, 3, and 100 mM, respectively. In experiment III the oocysts were diluted in a 3 mM $MgCl_2$ solution. Corresponding ionic strengths *I* are reported in Table 1. All experiments were conducted at neutral pH. The eluted fraction (the ratio of the eluted versus injected oocysts) ranged from 11% to 51% (Table 1).

[46] All measured BTCs show the distinct five-period behavior discussed in the introduction. A significant drop in concentration occurs after termination of the oocyst injection and prior to the onset of tailing. As ionic strength increases from very low values (0.01 mM) to typical drinking water concentrations (3 mM), peak concentration and total oocyst elution decrease significantly (by more than half an order of magnitude). A further decrease is observed for 10 mM NaCl concentrations (not shown). Peak concentrations in the 3 mM $MgCl_2$ solution and in the 100 mM NaCl solution are nearly as high as in the lower ionic strength experiments, suggesting no strong correlation between filtration of oocysts and ionic strength above levels of the 3 mM NaCl solution. On the other hand, with increasing *I*, the onset of tailing (transition from period D to E) occurs

Table 1. Experiments Characteristics and Best Fit Parameters for Models (11) and (4)

	θ	I, M	$\bar{f}$	α	λ	Λ	β	c	k_f	k_r
I	0.294	1×10^{-5}	0.1500	2×10^{-4}	0.9822	0.20	0.35	1.0	2×10^{-2}	1×10^{-1}
II	0.309	3×10^{-3}	0.5137	2×10^{-4}	2.1361	0.45	0.20	1.0	6.75×10^{-2}	1.5×10^{-1}
III	0.298	9×10^{-3}	0.2149	2×10^{-4}	1.5144	0.35	2×10^{-2}	0.98	7×10^{-4}	2×10^{-2}
IV	0.298	1×10^{-1}	0.1112	2×10^{-4}	1.0641	0.30	1×10^{-3}	0.96	9×10^{-4}	3×10^{-3}

later and hence at lower concentrations. The slope of the tail is also flatter at higher ionic strength.

[47] The parameters of the CTRW filtration model, equation (11), are determined by the following procedure.

[48] The dispersivity, α, is obtained by fitting the breakthrough curve for the bromide experiment to the ADE.

[49] The filtration coefficient λ represents the fraction of irreversibly sorbed oocysts [*Bolster et al.*, 1998] and is computed by taking the ratio of total oocyst mass eluted to total oocyst mass injected:

$$\lambda = -\ln(f) + \alpha \ln\left(f^2\right) \tag{15}$$

where f is the recovered eluted fraction. The total oocyst mass eluted for a given experiment is computed by stepwise integration of the experimental breakthrough curves and by averaging the values of the two replicate experiments. Note that λ is obtained independent of the particular shape of the BTC or of the specific height of the peak concentration.

[50] The sticking coefficient Λ is obtained by fitting period C of the BTC (breakthrough plateau) to the measured data. The parameters β and, if the slope decay is slower than t^{-1}, the parameter c are obtained by fitting the slope of the model tail to period E of the BTC.

[51] For comparison, we also fit the RADE filtration equations (4) to the measured curves. The filtration coefficient λ, the dispersivity α, and the retardation coefficient $R = 1 + \Lambda$ are identical to those used in the CTRW filtration model. The only parameter fitted separately is the first-order detachment rate k_r, which is obtained by fitting the location of the tailing transition point (period D to period E) and the early part of the tail (period E).

[52] With the CTRW model, excellent fitting results are obtained for the four *C. parvum* BTCs (Figure 3). The dispersivity obtained from the bromide experiment provides excellent prediction of the dispersive behavior of the oocysts in all experiments. The model accurately captures peak concentrations and the falling limb (period D) of the initial part of the BTC. Most importantly, the CTRW filtration model predicts the observed power law tailing over several orders of magnitude in elution time. The model does a good job of representing the duration of period D (falling limb), the onset of transition from period D to E, and the vertical location of the tail in period E, despite the fact that none of these variables are included in the fitting procedure. The model adequately captures these BTC characteristics without additional parametric control. The slope of the rising and falling limbs (periods B and D) of the BTC are well matched by the model, indicating that this particular phase of the transport is dominated by a classical ADE that can be independently determined using a conservative tracer.

[53] Small values of the ionic strength correspond to nonvanishing values for β (experiments I and II). For these two experiments, the power law tailing is preserved (and presumably infinite), hence $c = 1$. With divalent ion solution, 3 mM $MgCl_2$ instead of 3 mM NaCl, (experiment III in Figure 3) the best fit value of β is very close to zero. Near-zero β indicate dominance of power law behavior ($0 < \beta < 1$) and a tail characterized by a time decay slightly slower than t^{-1}. Increasing ionic strength I causes a decrease in the height of the energy barrier and an increase in the depth of the secondary minimum, thereby enhancing the deposition rates and limiting the escape rates [*Hahn and O'Melia*, 2004]. This implies that, at high ionic strengths, the transitions are dominated by a single reverse sorption rate. The slower than t^{-1} decay of the tail is particularly pronounced in the experiment with 100 mM NaCl. The sticking coefficient Λ varied slightly with ionic strength and is always between 0.2 and 0.35 (retardation factor varying from 1.2 to 1.35).

[54] The classic reactive ADE filtration model with first-order sorption-desorption kinetics (RADE model) is nearly identical to the CTRW filtration model during the early part of the breakthrough curve (periods A–D). The RADE formulation, however, fails to capture the characteristics of the power tail in the late part of the BTC (period E, Figure 3, dashed lines). The exponential decay of the RADE model BTC does not allow for adequate prediction of the long-term elution of oocysts. It either predicts the early most part of the tail accurately, but then quickly drops off, or it overpredicts the early part of the tail and underpredicts the late part of the tail. The RADE filtration model results would suggest that oocyst elution terminates to nondetectable levels after only a few tens of pore volumes, two orders of magnitude earlier than measured. This inconsistency is often ignored because the two models appear nearly identical when plotted on a linear-linear scale for experiments involving only a few pore volumes, but becomes quite important when the late time behavior is considered.

[55] Furthermore, currently used automatic fitting programs [*Toride et al.*, 1995] emphasize a good fit to the peak concentration (period C) but not to the tail (period E) due to the weighting of the error by the predicted concentration. Such a weighting scheme is inadequate for properly fitting the (low concentration) power law tail of long-elution BTCs and would not be capable of distinguishing a fit of the data to the CTRW filtration model from a fit to the RADE filtration model.

[56] Both models suggest that the total mass eluted (as expressed by λ) is often significantly greater than that included in the initial peak. Peak concentrations are therefore not suitable to predict total oocyst retention. The peak concentration masks the fact that significant remobilization may occur during and after the main breakthrough.

[57] Note that the CTRW filtration model does not replace nor invalidate the classic clean bed filtration model, as defined, e.g., by *Rajagopalan and Tien* [1976] or *Tufenkji and Elimelech* [2004]. The collector efficiency, η, can be computed from physical dimensions of the oocysts and the porous medium. Given the value for η for our experiments and given the λ obtained from the eluent oocyst mass, we obtain collision efficiencies, α_c ranging from 0.03 to 0.08, comparable to those found previously for bacteria [*Harvey and Garabedian*, 1991] and *C. parvum*. Short experiments, however, overestimate the collision efficiency as pointed out by *Harter et al.* [2000], who showed that the total mass eluted in the tail after the initial breakthrough peak can be more than one order of magnitude larger than the amount of mass eluted during the initial breakthrough.

[58] The comparison of the RADE and the CTRW filtration models highlights the strength of the CTRW filtration model. Excellent fits of the entire BTC behavior can be obtained by using the same parameter estimation

procedure that has been used for the RADE model parameters. Effective pore volumes are obtained from column data and dispersivity is obtained from an independent bromide experiment. The λ parameter can be estimated using clean bed filtration theory and an approximate value of the collision efficiency α_c. In the CTRW filtration model, the only fitting parameters are Λ and β and, possibly, c. The fitting parameter for the RADE model are k_r, and $k_f = k_r \Lambda$.

[59] A variety of laboratory column experiments have been conducted to estimate k_f and k_r using the RADE filtration model in (4), and the results have been used to forecast breakthrough curves at larger scale. However, even though the RADE filtration model has been fit observed data, the scalability of k_f and k_r has not been investigated. Similarly, the scalability of Λ, β and c is an open research question. Also, whether and how (2) can be used as a predictive tool to determine λ in the CTRW or RADE filtration models and to which degree the collision efficiency η in (2) controls Λ and β in the CTRW filtration model or λ, k_f, and k_r in the RADE filtration model remains the subject of future research. Regardless, the CTRW filtration model (like the RADE filtration model) may be used to predict BTCs for scenarios under different input concentrations in the same system. For example, once experiments for model calibration are completed, the CTRW filtration model can be used to predict future events for different input concentrations from an initial event to which parameters are fitted. Future work needs to address limits of this model at high biocolloid concentration.

5. Conclusions

[60] We present a set of laboratory experimental breakthrough curves that show late time elution of bromide and *C. parvum* oocysts from a quartz sand column over several thousand pore volumes past the initial injection. The experiments were conducted for a range of chemical compositions of the carrying solution. The oocyst BTCs exhibit anomalous (non-Fickian) tailing which cannot be explained by current filtration theories. A new filtration transport model based on the CTRW formalism accounts for heterogeneities that occur at multiple scales in the system. The model demonstrates that physicochemical heterogeneities at the scale of the transported colloids, collector grains surfaces, and pore size have a major impact on the attachment and detachment behavior of the oocysts at the macroscopic scale of the column experiments.

[61] The range of attachment and detachment rates generated by these scale processes is modeled by a power law probability distribution function that may eventually turn into a slower than t^{-1} decay by means of a an adjustable parameter. The resulting PDE equation is nonlocal in time, i.e., takes the form of a convolution between a time memory function and the classical filtration equation. The resulting model has the same number of fitting parameters as the RADE filtration model with first-order sorption-desorption yet provides substantially better simulations of the experimental results.

[62] The model enables us to distinguish between the effects of pore geometry disorder and particle surface heterogeneity that manifests itself in the non-Fickian tailing. We show that homogeneously packed sand columns yield nonideal transport behavior due to pore geometry disorder, as shown in the tail of the bromide BTC. However, the degree of physicochemical disorder completely overwhelms the geometric disorder, as shown in the degree of power law tailing of the *C. parvum* BTC. We show that the classic ADE is sufficiently accurate to represent processes controlling the advective-dispersive flux contributions to oocyst transport in homogeneously packed sand columns. It does not, however, accurately represent processes controlling the late time tailing behavior.

[63] Our *C. parvum* experiments indicate a decrease in initial breakthrough concentration between very low and low ionic strengths. As ionic strength increases further, peak concentrations do not continue to decrease, but the the slope of the BTC tail decreases with increasing I and becomes slower than t^{-1} for very large values of I. The dispersivity parameter is not affected by changes in I and is shown to be identical to that obtained from passive tracer experiments. The filtration coefficient λ is completely determined by the eluted recovery fraction and can be estimated using existing bed filtration models. However, the experiment must be conducted for a sufficiently long period of time and the analytical methods must allow for observation of the concentration decrease in the BTC over several orders of magnitude.

[64] Finally, we note that the application of the proposed model to *C. parvum* serves only as an example. In principle, this model is applicable to a wide range of colloid and biocolloid transport phenomena including virus and bacteria transport in groundwater and the assessment of colloid-facilitated transport of contaminants in groundwater.

[65] **Acknowledgments.** This research was supported by grant 2001-35102-10773 of the USDA NRICGP. This work was also conducted in part under the auspices of the Bernice Barbour Communicable Disease Laboratory, with financial support from the Bernice Barbour Foundation, Hackensack, New Jersey, as a grant to the Center of Equine Health, University of California, Davis. The authors thank Tom Young for the availability of the ICP-MS. We thank Marco Dentz and two anonymous reviewers for constructive comments.

References

Albinger, O., B. K. Biesemeyer, R. G. Arnold, and B. E. Logan (1994), Effect of bacterial heterogeneity on adhesion to uniform collectors by monoclonal populations, *FEMS Microbiol. Lett.*, *124*, 321–326.

Arrowood, M. J., and C. Sterling (1987), Isolation of *Cryptosporidium* oocysts and sporozoites using discontinuous sucrose and isopycnic Percoll gradients, *J. Parasitol.*, *73*, 314–319.

Atwill, E. R., B. Hoar, M. das Gracas Cabral Pereira, K. W. Tate, F. Rulofson, and G. Nader (2003), Improved quantitative estimates of low environmental loading and sporadic periparturient shedding of *Cryptosporidium parvum* in adult beef cattle, *Appl. Environ. Microbiol.*, *69*, 4604–4610.

Baygents, J. C., J. R. J. Glynn, O. Albinger, B. K. Biesemeyer, K. L. Ogden, and R. G. Arnold (1998), Variation of surface charge density in monoclonal bacterial populations: Implications for transport through porous media, *Environ. Sci. Technol.*, *32*, 1596–1603.

Berkowitz, B., and H. Scher (1995), On characterization of anomalous dispersion in porous and fractured media, *Water Resour. Res.*, *31*, 1461–1466.

Berkowitz, B., J. Klafter, R. Metzler, and H. Scher (2002), Physical pictures of transport in heterogeneous media: Advection-dispersion, random walk and fractional derivative formulations, *Water Resour. Res.*, *38*(10), 1191, doi:10.1029/2001WR001030.

Berkowitz, B., A. Cortis, M. Dentz, and H. Scher (2006), Modeling non-Fickian transport in geological formations as a continuous time random walk, *Rev. Geophys.*, *44*, RG2003, doi:10.1029/2005RG000178.

Bolster, C. H., G. M. Hornberger, A. L. Mills, and J. L. Wilson (1998), A method for calculating bacterial deposition coefficients using the fraction of bacteria recovered from laboratory columns, *Environ. Sci. Technol.*, *32*, 1329–1332.

Bolster, C. H., A. L. Mills, G. M. Hornberger, and J. S. Herman (1999), Spatial distribution of deposited bacteria following miscible displacement experiments in intact cores, *Water Resour. Res.*, *35*, 1797–1807.

Bradford, S. A., and M. Bettahar (2005), Straining, attachment, and detachment of *Cryptosporidium* oocysts in saturated porous media, *J. Environ. Qual.*, *34*, 469–478.

Bradford, S., and J. Schijven (2002), Release of *cryptosporidium* and *giardia* from dairy calf manure: Impact of solution salinity, *Environ. Sci. Technol.*, *36*, 3916–3923.

Camesano, T., and B. Logan (1998), Influence of fluid velocity and cell concentration on the transport of motile and non-motile bacteria in porous media, *Environ. Sci. Technol.*, *32*, 1699–1708.

Camesano, T. A., K. M. Unice, and B. E. Logan (1999), Blocking and ripening of colloids in porous media and their implications for bacterial transport, *Colloids Surf. A*, *160*, 291–308.

Cortis, A., and B. Berkowitz (2004), Anomalous transport in "classical" soil and sand columns, *Soil Sci. Soc. Am. J.*, *68*, 1539.

Cortis, A., Y. Chen, H. Scher, and B. Berkowitz (2004a), Quantitative characterization of pore-scale disorder effects on transport in "homogeneous" granular media, *Phys. Rev. E*, *70*, 041108.

Cortis, A., C. Gallo, H. Scher, and B. Berkowitz (2004b), Numerical simulation of non-Fickian transport in geological formations with multiple-scale heterogeneities, *Water Resour. Res.*, *40*, W04209, doi:10.1029/2003WR002750.

Cote, M. M., M. B. Emelko, and N. R. Thomson (2002), Factors influencing prediction of *Cryptosporidium parvum* removal in riverbank filtration systems: Focus on filtration, paper presented at Water Quality Technology Conference, Am. Water Works Assoc., Seattle, Wash., 11–13 Nov.

de Marsily, G. (1986), *Quantitative Hydrogeology: Groundwater Hydrology for Engineers*, Elsevier, New York.

Dentz, M., A. Cortis, H. Scher, and B. Berkowitz (2004), Time behavior of solute transport in heterogeneous media: Transition from anomalous to normal transport, *Adv. Water Resour.*, *27*, 155–173, doi:10.1016/j.advwatres.2003.11.002.

Ginn, T., B. D. Wood, K. E. Nelson, T. D. Scheibe, E. M. Murphy, and T. P. Clement (2002), Processes in microbial transport in the natural subsurface, *Adv. Water Resour.*, *25*, 1017–1042.

Hahn, M. W., and C. R. O'Melia (2004), Deposition and reentrainment of Brownian particles in porous media under unfavorable chemical conditions: Some concepts and applications, *Environ. Sci. Technol.*, *5*, 1105–1112, doi:10.1021/es60058a005.

Hancock, C. M., J. B. Rose, and M. Callahan (1998), *Crypto* and *Giardia* in U.S. groundwater, *J. Am. Water Works Assoc.*, *90*(3), 58–61.

Harp, J. A., P. Jardon, E. R. Atwill, M. Zylstra, S. Checel, J. P. Goff, and C. Desimone (1996), Field testing of prophylactic measures against *Cryptosporidium parvum* infection in calves in a California dairy herd, *Am. J. Vet. Res.*, *57*, 1586–1588.

Harter, T., S. Wagner, and E. R. Atwill (2000), Colloid transport and filtration of *Cryptosporidium parvum* in sandy soils and aquifer sediments, *Environ. Sci. Technol.*, *38*, 210–220.

Harvey, R. W., and S. P. Garabedian (1991), Use of colloid filtration theory in modeling movement of bacteria through a contaminated sandy aquifer, *Environ. Sci. Technol.*, *25*, 178–185, doi:10.1021/es00013a021.

Hou, L., X. Li, L. Dunbar, R. Moeller, B. Palermo, and E. R. Atwill (2004), Neonatal mice infectivity of intact *Cryptosporidium parvum* oocysts isolated after optimized in vitro excystation, *Appl. Environ. Microbiol.*, *70*, 642–646.

Israelachvili, J. N. (1991), *Intermolecular and Surface Forces*, Elsevier, New York.

Jiménez-Hornero, F. J., J. V. Giráldez, A. Laguna, and Y. Pachepsky (2005), Continuous time random walks for analyzing the transport of a passive tracer in a single fissure, *Water Resour. Res.*, *41*, W04009, doi:10.1029/2004WR003852.

Johnson, P. R., N. Sun, and M. Elimelech (1996), Colloid transport in geochemically heterogeneous porous media: Modeling and measurements, *Environ. Sci. Technol.*, *30*, 3284–3293.

Johnson, W. P., K. A. Blue, B. E. Logan, and R. G. Arnold (1995), Modeling bacterial detachment during transport through porous media as a residence-time-dependent process, *Water Resour. Res.*, *31*, 2649–2658.

Johnson, W. P., X. Li, and M. Tong (2005), Colloid retention behavior in environmental porous media challenges existing theory, *Eos Trans. AGU*, *86*, 179–180.

Kuznar, Z., and M. Elimelech (2004), Adhesion kinetics of viable *Cryptosporidium parvum* oocysts to quartz surfaces, *Environ. Sci. Technol.*, *38*, 6839–6845.

Kuznar, Z., and M. Elimelech (2005), Role of surface proteins in the deposition kinetics of *Cryptosporidium parvum* oocysts, *Langmuir*, *21*, 710–716.

Lisle, J. T., and J. B. Rose (1995), *Cryptosporidium* contamination of water in the USA and UK: A mini-review., *J. Water Supply Res. Technol.*, *44*, 103–117.

Logan, B. E., D. G. Jewett, R. G. Arnold, E. J. Bouwer, and C. R. O'Melia (1995), Clarification of clean-bed filtration models, *J. Environ. Eng.*, *121*, 869–873, doi:10.1061/(ASCE)0733-9372(1995)121:12(869).

Margolin, G., M. Dentz, and B. Berkowitz (2003), Continuous time random walk and multirate mass transfer modeling of sorption, *Chem. Phys.*, *295*, 71–80.

Martin, M. J., B. E. Logan, W. P. Johnson, D. G. Jewett, and R. G. Arnold (1996), Scaling bacterial filtration rates in different sized porous media, *J. Environ. Eng.*, *122*, 407–415.

McDowell-Boyer, L., J. R. Hunt, and N. Sitar (1986), Particle transport through porous media, *Water Resour. Res.*, *22*, 1901–1921.

Okhuysen, P., C. L. Chappell, J. H. Crabb, C. R. Sterling, and H. L. DuPont (1999), Virulence of three different *Cryptosporidium parvum* isolates for healthy adults, *J. Infect. Dis.*, *180*, 1275–1281.

Rajagopalan, R., and C. Tien (1976), Trajectory analysis of deep bed filtration with the sphere-in-cell porous media model, *AIChE J.*, *3*, 523–533.

Redman, J. A., M. K. Estes, and S. B. Grant (2001a), Resolving macroscale and microscale heterogeneity in virus filtration, *Colloids Surf. A*, *191*, 57–70.

Redman, J. A., S. B. Grant, T. M. Olson, and M. K. Estes (2001b), Pathogen filtration, heterogeneity, and the potable reuse of watewater, *Environ. Sci. Technol.*, *35*, 1798–1805.

Redman, J. A., S. L. Walker, and M. Elimelech (2004), Bacterial adhesion and transport in porous media: Role of the secondary energy minimum, *Environ. Sci. Technol.*, *38*, 1777–1785.

Ren, J., and A. Packman (2002), Effects of particle size and background water composition on stream-subsurface exchange of colloids, *J. Environ. Eng.*, *128*, 624–634.

Robertson, L. J., A. T. Campbell, and H. V. Smith (1992), Survival of *Cryptosporidium parvum* oocysts under various environmental pressures, *Appl. Environ. Microbiol.*, *58*, 3494–3500.

Ryan, J. N., and M. Elimelech (1996), Colloid mobilization and transport in groundwater, *Colloids Surf. A*, *107*, 1–56.

Schijven, J. F., S. A. Bradford, and S. Yang (2004), Release of *Cryptosporidium* and *Giardia* from dairy cattle manure: Physical factors, *J. Environ. Qual.*, *33*, 1499–1508.

Song, L., P. R. Johnson, and M. Elimelech (1994), Kinetics of colloid deposition onto heterogeneously charged surfaces in porous media, *Environ. Sci. Technol.*, *28*, 1164–1171.

Toride, N., F. Leij, and M. van Genuchten (1995), The CXTFIT code for estimating transport parameters from laboratory or field tracer experiments, version 2.0, *Res. Rep. 137*, U.S. Salinity Lab., Riverside, Calif.

Tufenkji, N., and M. Elimelech (2004), Correlation equation for predicting single-collector efficiency in physicochemical filtration in saturated porous media, *Environ. Sci. Technol.*, *38*, 529–536.

Tufenkji, N., G. F. Miller, J. N. Ryan, R. W. Harvey, and M. Elimelech (2004), Transport of *Cryptosporidium* oocysts in porous media: Role of straining and physicochemical filtration, *Environ. Sci. Technol.*, *38*, 5932–5938.

Walker, M. J., C. D. Montemagno, and M. B. Jenkins (1998), Source water assessment and nonpoint sources of acutely toxic contaminants: A review of research related to survival and transport of *Cryptosporidium parvum*, *Water Resour. Res.*, *34*, 3383–3392.

Xiao, L., L. Escalante, C. Yang, I. Sulaiman, A. A. Escalante, R. J. Montali, R. Fayer, and A. A. Lal (1999), Phylogenetic analysis of *Cryptosporidium* parasites based on the small-subunit rRNA gene locus, *Appl. Environ. Microbiol.*, *65*, 1578–1583.

Yao, K.-M., M. T. Habibian, and C. R. O'Melia (1971), Water and waste water filtration: Concepts and applications, *Environ. Sci. Technol.*, *5*, 1105–1112, doi:10.1021/es60058a005.

E. R. Atwill and L. Hou, Department of Population Health and Reproduction, Veterinary Medicine Teaching and Resource Center, University of California, Davis, Tulare, CA 93274, USA.

A. Cortis, Earth Science Division, Lawrence Berkeley National Laboratory, 1 Cyclotron Road, Berkeley, CA 94720, USA. (acortis@lbl.gov)

P. G. Green, Department of Civil and Environmental Engineering, University of California, Davis, CA 95616, USA.

T. Harter, Department of Land, Air, and Water Resources, University of California, Davis, CA 95616, USA.

A. I. Packman, Department of Civil and Environmental Engineering, Northwestern University, Evanston, IL 60208, USA.